Article

Cell Systems

Longitudinal RNA-Seq Analysis of Vertebrate Aging Identifies Mitochondrial Complex I as a Small-Molecule-Sensitive Modifier of Lifespan

Graphical Abstract

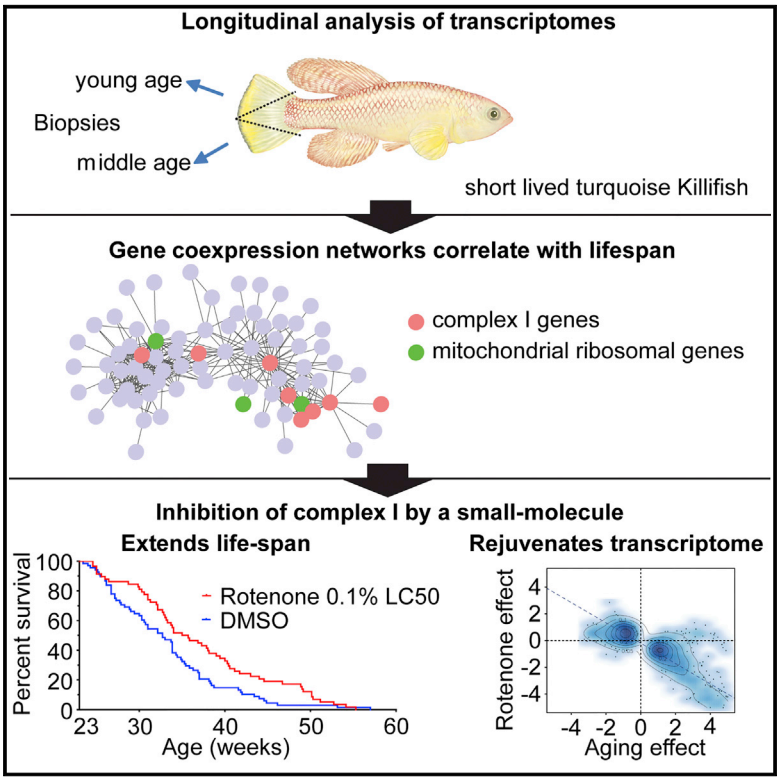

Authors

Mario Baumgart, Steffen Priebe, Marco Groth, ..., Reinhard Guthke, Matthias Platzer, Alessandro Cellerino

Correspondence

alessandro.cellerino@sns.it

In Brief

A longitudinal transcriptome analyses was performed in a short-lived fish by taking two fin clips during early adult life to correlate gene expression with lifespan. Gene-coexpression network analysis identified complex I of the mitochondrial respiratory chain as a hub for negative correlation with lifespan, and its pharmacological inhibition prolonged lifespan and rejuvenated the transcriptome.

Highlights

- Longitudinal transcriptome correlation with lifespan in a short-lived vertebrate
- Shorter- and longer-lived individuals differ in transcriptome profiles at a young age
- Mitochondrial complex I identified as a hub for negative correlation with lifespan
- Inhibition of complex I prolongs lifespan and rejuvenates the transcriptome

Accession Numbers

GSE52462
GSE66362
GSE66712

Baumgart et al., 2016, Cell Systems 2, 122–132
February 24, 2016
http://dx.doi.org/10.1016/j.cels.2016.01.014

OPEN ACCESS
CellPress

Cell Systems
Article

Longitudinal RNA-Seq Analysis of Vertebrate Aging Identifies Mitochondrial Complex I as a Small-Molecule-Sensitive Modifier of Lifespan

Mario Baumgart,[1,6] Steffen Priebe,[2,6] Marco Groth,[1,6] Nils Hartmann,[1,6] Uwe Menzel,[2] Luca Pandolfini,[3,7] Philipp Koch,[1] Marius Felder,[1] Michael Ristow,[4] Christoph Englert,[1,5] Reinhard Guthke,[2] Matthias Platzer,[1] and Alessandro Cellerino[1,3,*]
[1]Leibniz Institute on Aging-Fritz Lipmann Institute (FLI), Beutenbergstraße 11, 07745 Jena, Germany
[2]Leibniz Institute for Natural Product Research and Infection Biology-Hans Knöll Institute (HKI), Beutenbergstraße 11a, 07745 Jena, Germany
[3]Scuola Normale Superiore, Laboratory of Biology, c/o Istituto di Biofisica del CNR, via Moruzzi 1, 56124 Pisa, Italy
[4]Energy Metabolism Laboratory, ETH Zürich (Swiss Federal Institute of Technology), Schorenstrasse 16, 8603 Schwerzenbach-Zürich, Switzerland
[5]Faculty of Biology and Pharmacy, Friedrich Schiller University Jena, 07743 Jena, Germany
[6]Co-first author
[7]Present address: Wellcome Trust/CRUK Gurdon Institute, University of Cambridge, Tennis Court Rd, Cambridge CB2 1QN, UK
*Correspondence: alessandro.cellerino@sns.it
http://dx.doi.org/10.1016/j.cels.2016.01.014

SUMMARY

Mutations and genetic variability affect gene expression and lifespan, but the impact of variations in gene expression within individuals on their aging-related mortality is poorly understood. We performed a longitudinal study in the short-lived killifish, *Nothobranchius furzeri*, and correlated quantitative variations in gene expression during early adult life with lifespan. Shorter- and longer-lived individuals differ in their gene expression before the onset of aging-related mortality; differences in gene expression are more pronounced early in life. We identified mitochondrial respiratory chain complex I as a hub in a module of genes whose expression is negatively correlated with lifespan. Accordingly, partial pharmacological inhibition of complex I by the small molecule rotenone reversed aging-related regulation of gene expression and extended lifespan in *N. furzeri* by 15%. These results support the use of *N. furzeri* as a vertebrate model for identifying the protein targets, pharmacological modulators, and individual-to-individual variability associated with aging.

INTRODUCTION

Aging results from accumulation of molecular and cellular damage and leads to progressive physiological failure and an increase in mortality. Differences in aging and lifespan between individuals of the same species are influenced by intrinsic (both heritable and random variation) and extrinsic factors, such as nutrition (de Cabo et al., 2014; Herndon et al., 2002; Pincus et al., 2011; Rea et al., 2005; Shen et al., 2014). Well-established single-gene mutations can increase longevity in model organisms (Bartke, 2011; Fontana et al., 2010; Gems and Partridge, 2013; Lee et al., 2003) and some *loci* influencing human or murine lifespan have been identified (Beekman et al., 2013; Broer et al., 2015; Deelen et al., 2014; Houtkooper et al., 2013; Willcox et al., 2008).

While genetic heterogeneity clearly influences lifespan, the relationship between non-genetic variation and the specific age-related phenotypes observed in individuals is not well understood. To the best of our knowledge, all available studies on individual random variation and aging have been performed in the roundworm, *Caenorhabditis elegans*. Pioneering studies showed that the expression level of heat-shock proteins can predict individual lifespan, and this trait is not heritable (Rea et al., 2005). This observation demonstrates that variability in the absence of genetic heterogeneity may influence the lifespans of individuals. Later studies identified the expression level of the miR-71 microRNA (Pincus et al., 2011) and the frequency of "mitoflashes" during an individual's early adult life (Shen et al., 2014) as predictors of lifespan. Accordingly, knock down of mitochondrial proteins during development is necessary and sufficient to cause life-extension in *C. elegans* (Dillin et al., 2002b; Houtkooper et al., 2013). Taken together, these studies suggest that conditions favoring longevity may be laid out during development and early adult life.

Historically, the extension of similar studies to vertebrates has been hampered by the lifespan of the available model organisms. In the last decade, we developed the annual African turquoise killifish (*Nothobranchius furzeri*), the shortest-lived vertebrate that can be cultured in captivity (Valdesalici and Cellerino, 2003), into a model organism for aging studies. *N. furzeri* is particularly suited to longitudinal studies: the maximum lifespan of this species is 3–12 months, depending on the genetic background (Terzibasi et al., 2008). The highly inbred strain GRZ can have a lifespan span as short as 3 months, while strains collected more recently, such as the MZM-0410 strain used in this paper, have longer lifespans. *N. furzeri* is responsive to interventions that prolong the lifespan of other model organisms such as temperature, calorie restriction, and resveratrol (Terzibasi et al., 2009; Valenzano et al., 2006a, 2006b), and many aspects of vertebrate aging are observed in *N. furzeri* (Cellerino et al., 2015), including mitochondrial

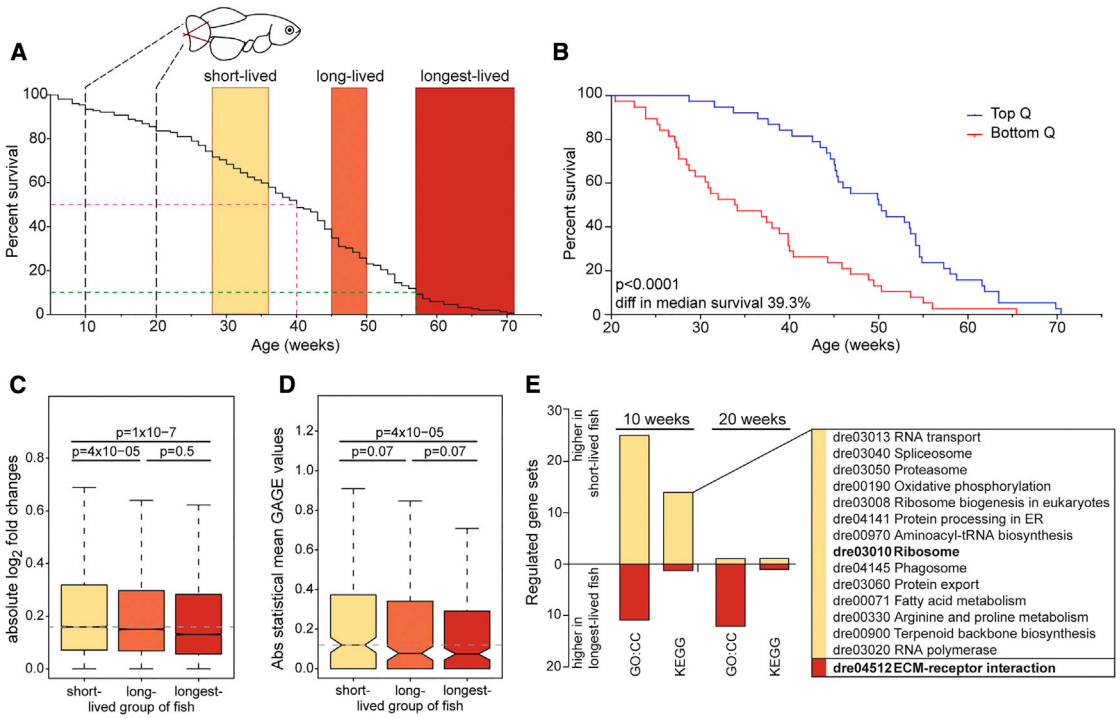

Figure 1. Survivorship of the Study Population, Correlation of Growth Parameters with Lifespan, and Differences of Gene Expression among Groups with Diverging Lifespan

(A) Survivorship of the lifespan study population (n = 152). The red dashed line indicates the median survivorship, the dashed green line the 10% survivorship, the dashed black vertical lines indicate the sampling ages. The boxes indicate the lifespan intervals of the short-lived, longer-lived, and longest-lived groups, respectively.

(B) Differences in survival between the first and the last quartile of increase in body weight.

(C) Distribution of absolute $\log_2$ fold changes for 21,191 genes between 10 and 20 weeks in each of the three lifespan groups. Lines represent medians, boxes represent 25%–75% intervals, and whiskers represent 5%–95% intervals. Outliers are not shown. Differences in fold changes were tested by ANOVA.

(D) Distribution of absolute $\log_2$ statistical mean, a measure of up- or downregulation within a gene set, for all 136 annotated *D. rerio* KEGG pathways. Outliers are not shown. Differences in fold changes were tested by Wilcoxon-Mann-Whitney test.

(E) Number of DEG sets between the short-lived and the longest-lived group at 10 and 20 weeks. The inbox lists the differentially regulated KEGG pathways at 10 weeks; pathways in bold are also differentially regulated at 20 weeks.

See also Tables S1, S2, S3, S4, S5, S6, and S7.

dysfunction (Hartmann et al., 2011). RNA sequencing (RNA-seq)-based studies have demonstrated that the patterns of genome-wide transcript regulation in the *N. furzeri* brain mimic those observed in mammals (Baumgart et al., 2014), and new large-scale studies are facilitated by the recent sequencing of the *N. furzeri* genome (Reichwald et al., 2015; Valenzano et al., 2015).

Here, we perform a longitudinal study of gene expression in individual *N. furzeri* by obtaining two fin biopsies at two time points during early adult stage, then correlate the specific gene expression signatures observed in these individuals during early adult life with their age at death. To identify the most relevant genes expression signatures for lifespan determination, we generated a gene co-expression network using weighted gene co-expression network analysis (WGCNA) (Zhang and Horvath, 2005). This approach allows us to correlate gene modules with external variables (lifespan in this case) and identified central hubs in the network of longevity-related genes.

RESULTS

The lifespan of 152 male *N. furzeri,* strain MZM-0410, was recorded starting from week 5 (sexual maturity). Simultaneously, we obtained two independent biopsies of the caudal fin at age 10 weeks and 20 weeks (corresponding to ~15% and ~30% of maximum lifespan) from each individual that reached 20 weeks (n = 130). Fins regenerate in fish, and this procedure is not likely to impair survival of the experimental fish. Median lifespan for the study groups was 40 weeks and 10% survivorship was 58 weeks (Figure 1A). We then selected 45 individuals based on the age of death divided into three groups of 15 individuals each: short-lived (age of death 28–36 weeks), long-lived (age of death 45–50 weeks), and longest-lived (age of death 57–71 weeks,). We excluded animals from analysis that died before 28 weeks of age because several of these animals show negative growth between 10 and 20 weeks (Tables S1 and S2), suggesting a disease or environmental component of mortality in the earliest-dying group. The shape of the survival curve is similar to what recorded in this wild-derived strain in previous experiments (e.g., Terzibasi et al., 2009), and the broad distribution of individual lifespans could be related to residual genetic heterozygosity known to be present in this newly inbred strain. We therefore analyzed heterozygosity genome-wide and found that the number of single nucleotide variations in MZM-0410 was 42 times higher than in the highly inbred strain GRZ (Table S3). The hatch dates

of the individuals were balanced in the three groups (Table S1) to eliminate cohort effects. For each individual, the following information was recorded: age at sexual maturity (i.e., time when nuptial livery was first visible), weight and length at 10 weeks, weight and length at 20 weeks, and increase in weight and length between 10 and 20 weeks (Tables S1 and S2). On the whole populations, growth was positively associated with lifespan (Figure 1D), but none of these parameters statistically correlated with age of death within the 45 individuals used for the study ($p > 0.4$, Pearson's correlation, for details and additional analysis, see Table S4). Within each sample, transcript abundance was quantified by RNA-seq using as reference the *N. furzeri* genome including 23,546 protein-coding genes (for mapping statistics, see Table S5). To filter low-expressed genes than give unreliable estimates of fold-changes, the 10% lowest expressed genes (based on reads per kilobase of transcript per million [RPKM] values) were eliminated from the analysis, and this resulted in 21,191 genes passing this filter.

For each of the 45 individuals, we normalized across samples using size factors estimated with DESeq2 (Love et al., 2014), then, for each of the 21,191 genes that passed the filter described above, we calculated the fold-changes in gene expression observed between the 10-week and 20-week biopsy. We then calculated the median absolute fold-changes in gene expression between 10 and 20 weeks for the short-, long-, and longest-lived groups of fish separately. We found that largest differences were observed in the short-lived fish and the smallest were observed in the longest-lived fish ($p = 10^{-7}$, Wilcoxon signed-rank test, Figure 1C). This demonstrates that the longest-lived fish, as a group, globally display the smaller modulations in gene expression as a function of age. We further tested the age-dependent expression observed in specific gene sets using all 136 *Danio rerio* (zebrafish) KEGG pathways as input and generally applicable gene enrichment (GAGE) analysis (Luo et al., 2009). The absolute statistical mean provided by GAGE is a measure of the cumulative fold-changes observed across samples within a given gene set; it was largest in the short-lived and smallest in longest-lived groups of fish ($p = 4 \times 10^{-5}$, Wilcoxon signed-rank test, Figure 1D). Further, the number of KEGG pathways differentially expressed between 10 and 20 weeks was largest in short-lived and smallest in longest-lived groups of fish (Table S6) confirming the result from the single-gene analysis that an individual fish will experience comparatively little changes in gene expression between 10 and 20 weeks of age if it will be among the longest-lived group.

Having characterized gene expression within groups of fish (as determined by age of death), we next characterized gene expression between groups of fish. Specifically, we tested whether short-lived and longest-lived fish differ either at 10 or at 20 weeks of age in the expression of specific gene sets and pathways by GAGE analysis using KEGG pathways and gene ontology:cellular component (GO:CC) as gene sets (Table S7). The number of KEGG pathways and GO:CC sets that were differentially expressed in a statistically significant manner between the short-lived and longest-lived groups of fish was 15 and 36, respectively, when global gene expression was characterized at 10 weeks (Figure 1E). By contrast, only two KEGG pathways were expressed in statistically different manner between the short-lived and longest-lived groups of fish at 20 weeks: dre03010 ribosome, which was higher expressed in short-lived as compared to longest-lived fish, and dre04512 ECM-receptor interaction, which was lower expressed in the shortest-lived fish.

Characterization of Age-Dependent Gene Expression

Our analysis demonstrated that the differences in gene expression between the short- and longest-lived fish are largest at the earliest time point, suggesting that non-genetic factors that contribute to age of death are present early in life. To provide a baseline for identifying these lifespan-determining factors within individuals, we first needed to characterize average age-dependent gene expression. We analyzed RNA-seq data from brain, skin, and liver samples of male animals of five age groups (5, 12, 20, 27, and 39 weeks) and five biological replicates for each age (Baumgart et al., 2014; Reichwald et al., 2015) (Figure S1; see also Table S8). We selected genes that were differentially expressed between the first and the last age groups (false discovery rate [FDR]-corrected $p < 0.05$, DESeq, and edgeR, for the 100 top differentially expressed genes, see Table S9). We analyzed to what extent each pair of consecutive temporal steps differ by plotting the number of differentially expressed genes for each pairwise comparison and each tissue separately. For all three tissues, the number of differentially expressed genes was highest for the comparison between 5 and 12 weeks, declined until 27 weeks, then increased between 27 and 39 weeks (Figure 2A).

To investigate common age-dependent regulation across tissues, we selected genes that were differentially expressed in at least two tissues (n = 6,449) and their expression profiles were clustered using fuzzy c-means clustering. The optimal number of four clusters was determined by the vote of 42 cluster validity indices including variations of the Dunn's and Davis-Boulduin's indices as well as more recent indices as described (Guthke et al., 2005). The age-dependent regulation was similar across tissues. A representative cluster is displayed in Figure 2B. The rest can be found in Figure S2 (see also Table S10). We identified the KEGG pathways differentially expressed as a function of age in brain, liver, and skin using GAGE and tested whether the expression level of the genes within the gene set was correlated with age (as originally suggested by Zahn et al., 2006, 2007). For each tissue, the majority of age-regulated pathways were shared with at least another tissue and nine KEGG pathways were age-regulated in all three tissues (Figure 2C; Table S11).

Next, we asked whether any of the nine age-regulated pathways shared by all three tissues where differentially expressed between the three lifespan groups. We observed that components of the dre03013 RNA transport pathway were expressed at lower levels in the longest-lived versus short-lived groups of fish when gene expression was characterized at 10 weeks (FDR = 0.00017, GAGE) (Figure 2C, left). The dre03010 ribosome pathway was expressed at lower levels in the longest-lived fish as compared to the short-lived fish at both 10 and 20 weeks of age (FDR = 0.014 and p = 0.048, respectively, GAGE) (Figure 2C, right). Moreover, both the starting values of dre03010 ribosome pathway expression and its fold-changes across time varied between groups of fish; fold-change amplitude was largest in the short-lived group. These data are reminiscent of Figure 1E and suggest that the correlations observed in the fin biopsies

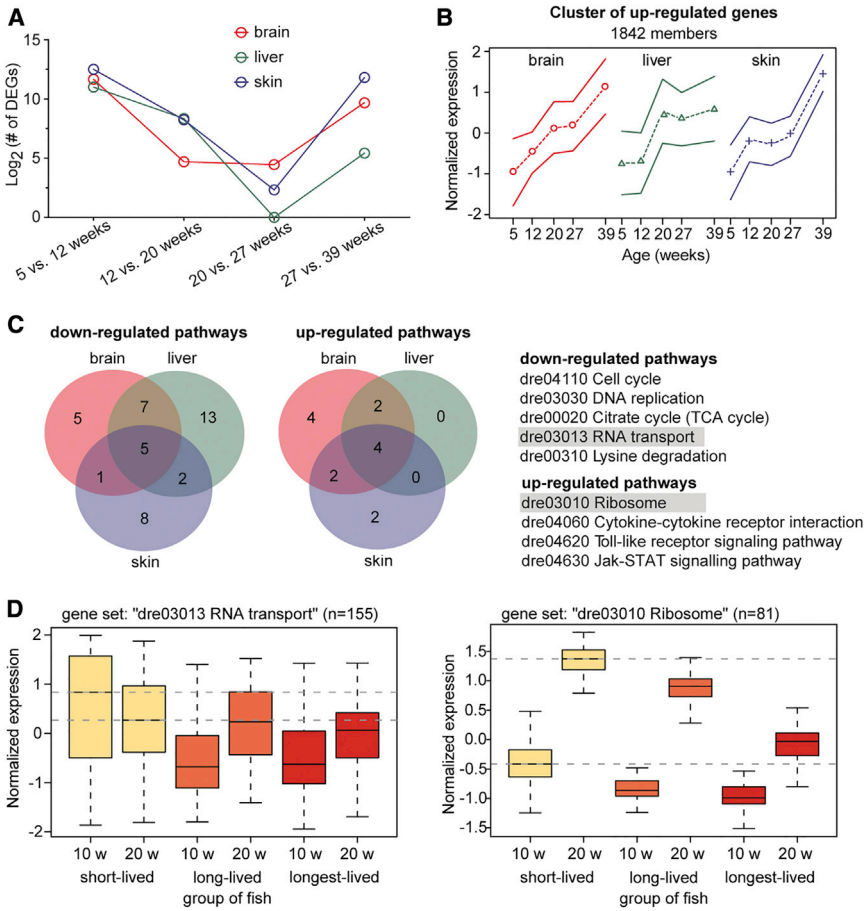

Figure 2. Characterization of Age-Dependent Gene Expression

(A) "Hourglass" pattern of age-dependent transcript modulation. The number of DEGs for each pair of consecutive temporal steps is reported in $\log_2$ scale for all three tissues. The number of DEGs is highest for the comparison between 5 and 12 weeks, abruptly declines and strongly increases for the comparison between 27 and 39 weeks.

(B) Fuzzy c-means clustering of DEGs in at least two out of three tissues, one representative cluster (for all clusters see Figure S2). The lines report cluster expression profiles in brain, liver, and skin, respectively. Points represent means, and lines represent confidence intervals. The expression of each gene was scaled to SD and centered to the mean for each of the three tissues separately. The number of genes in each cluster is reported on top of each graph. The optimal number of four was determined by the maximum of the cluster validation index.

(C) Overlap of age-regulated KEEG pathways. Generally applicable gene enrichment (GAGE) analysis using as input correlation of gene expression with age using values at 5, 12, 20, and 27 weeks. FDR-corrected $p < 0.05$. Values at 39 weeks were excluded because this time point is past median lifespan and may reflect selection effects.

(D) Normalized expression levels for all genes of the categories "dre03013 RNA transport" and "dre03010 ribosome." The gray dotted lines correspond to the median in group 1 at 10 and 20 weeks (w), respectively. Lines represent medians, boxes represent 25%–75% intervals, and whiskers represent 5%–95% intervals. Outliers are not shown.

See also Figures S1 and S2 and Tables S8, S9, S10, and S11.

between gene expression and age of death may be representative of similar correlations in other tissues.

Next, we investigated the relationship between age-dependent gene regulation and lifespan-associated gene expression. For all 21,191 genes passing our expression filter, we computed a correlation with age of death; this correlation was significant for 936 ($p < 0.05$, Spearman rank correlation). The expression of these genes was analyzed in brain, liver, and skin across time using fuzzy c-means clustering (Table S12). For the genes positively correlated with age of death (n = 248), all three clusters showed age-dependent downregulation in skin, whose profile of gene expression is very similar to fins (Figure S1), but differ in their regulation in the other two tissues.This association designates these genes as markers of skin biological age; functionally, they may oppose skin aging (Figure S3). The largest fraction of genes negatively correlated with lifespan (n = 688) were assigned to a cluster showing upregulation in all three tissues (38%, 261, Figure 3A) and are therefore markers of skin biological age; functionally, they may promote skin aging. The second cluster (36%, 251, Figure 3B) showed a U-shaped profile with a sharp decay between 5 and 12 weeks and upregulation at later time points in all three tissues. This behavior may indicate that these genes show different profiles in short- and longer-lived individual, and the population pattern may indicate higher mortality of those animals with early downregulation (see also Figure 2D, left). This cluster shows the highest enrichment for genes coding for proteins of the mitochondrial inner membrane (n = 20, GO:0005743, fold-enrichment = 7.2, $p = 1.3 \times 10^{-9}$, Fisher's exact test, Benjamini-Hochberg correction; Table S13). Examining the expression of all genes of this class (GO:0005743) as a function of age in the three lifespan groups showed that this gene set was expressed at lower levels in the longer living groups at 10 weeks (GAGE, FDR = 0.0078 and for short- versus longest-lived fish; Figure 3B, bottom). It should be noted that GO:0005743 was also detected with very high support as downregulated in a meta-analysis of age-dependent transcript regulation in mammals (de Magalhães et al., 2009). A third cluster shows a pattern that is not consistent across tissues (Figure 3C).

Identification of Co-regulated Genes that Are Associated with Age of Death

Network analysis is useful to identify genes that are putative hubs of gene co-regulation. Here, we applied the approach of weighted gene co-expression network analysis (WGCNA) (Zhang and Horvath, 2005). WGCNA groups genes into discrete modules based on their topological overlap within a network built from gene expression data. It also computes the eigengene of each module separately. The eigengene can then be correlated with an external variable, in our case, age of death. We used WGCNA to analyze the 936 genes correlated with age

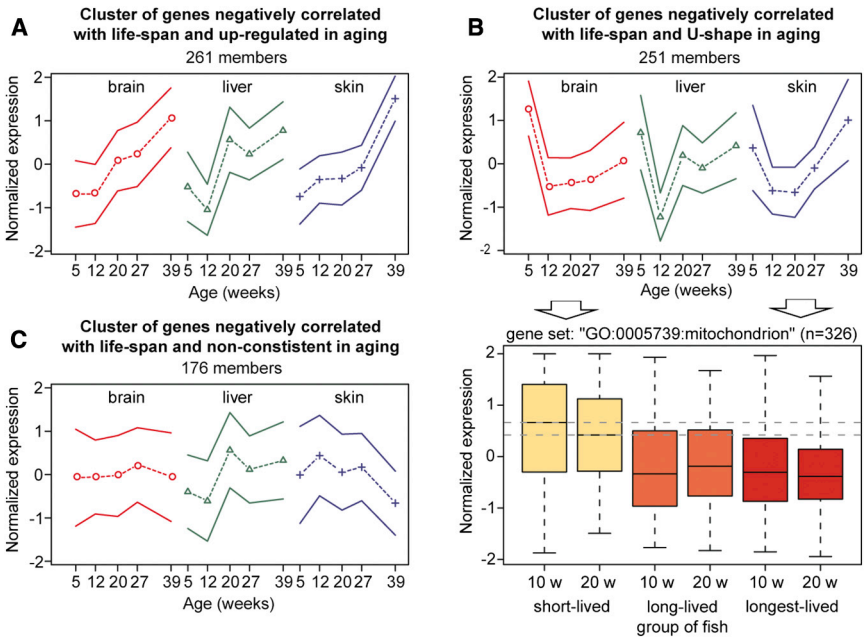

Figure 3. Temporal Clustering of Genes Correlated with Lifespan

(A and C) Fuzzy c-means clustering of 688 genes negatively correlated with lifespan. Lines report cluster expression profiles in brain, liver, and skin, respectively. Points represent means and lines represent confidence intervals. The expression of each gene was scaled to SD and centered to the mean for each of the three tissues separately.

(B) Normalized expression levels for all genes of the category "GO:0005743:mitochondrial inner membrane." The grey dotted lines correspond to the median in group 1 at 10 and 20 weeks (w), respectively. Lines represent medians, boxes represent 25%–75% intervals, and whiskers represent 5%–95% intervals. Outliers are not shown.

See also Figure S3 and Tables S12 and S13.

of death (Spearman correlation, $p < 0.05$). These genes were segmented into five modules, and for each of these modules, the correlation of the eigengene with age of death was computed (Figures 4A and S4; Table S14). The cluster membership for a gene in each module is defined as the correlation between the expression of a given gene and the eigengene of the module. Genes with the highest module membership (i.e., the best correlation with the module eigengene) can be considered as hubs. We focused our attention on the module 2 (149 genes; Table S14) that shows the largest absolute eigengene correlation with age of death (-0.45, $p = 10^{-5}$, Benjamini-Hochberg correction, Figure 4B) with top enrichments for complex I of the respiratory chain ($n = 6$, GO:0045271, $p = 6 \times 10^{-5}$, Fisher's exact test, Benjamini-Hochberg correction) and mitochondrial small ribosomal subunit ($n = 4$, GO:0005761, $p = 6 \times 10^{-5}$; Figure 4C; Table S15). Among the top ten hub genes (Table S16) are genes coding for NADH ubiquinone oxidoreductase A13 (NDUFA13) that is part of complex I of the electron transport chain and mitochondrial ribosomal protein S15 (MRPS15). Analysis of the gene network in this module revealed that genes coding for NDUFs and MRPs are tightly co-regulated (Figure 4D). This finding is consistent with mouse studies where *Mrps5* expression strongly correlates with expression of oxidative phosphorylation proteins (Houtkooper et al., 2013), and expression of MRPs is negatively correlated with lifespan across mouse strains (Houtkooper et al., 2013).

Activity of Respiratory Chain Complex I Affects Lifespan

In order to test whether relevance of complex I for lifespan determination could be observed in a different context, we performed two different experiments. First, we analyzed RNA-seq data from skin samples of five animals of the shorter-lived strain GRZ at the median lifespan of this strain; 12 weeks of age (Reichwald et al., 2015; Terzibasi et al., 2008). These data were compared to samples generated from MZM-0410 animals of the same age. GAGE analysis detected two KEGG pathways with higher expression in GRZ, including dre00190 oxidative phosphorylation (FDR = 9×10^{-12}), which contains complex I genes. This provides an independent confirmation that higher activity of complex I is associated with short lifespan.

Second, complex I of the respiratory chain can be potently inhibited by small molecules, such as rotenone (ROT) (Singer and Ramsay, 1994). This allowed us to ask directly whether partial inhibition of the respiratory chain affects fish lifespan. We treated *N. furzeri* MZM-0410 chronically with 15 pM and 150 pM ROT in the water, corresponding to 0.1% and 1% of the median lethal concentration (LC_{50}) for *N. furzeri*, respectively, starting at age 23 weeks. The lower concentration induced lifespan extension (log-rank test, $p = 0.0181$) but the higher concentration induced lifespan shortening (log-rank test, $p < 0.0001$, Figure 5).

Five animals treated with 15 pM ROT were taken after 4 weeks of treatment and RNA-seq was performed from brain, liver, and skin samples. These were compared with animals of the same age treated with vehicle and with animals treated with vehicle for 4 weeks starting at age 5 weeks (young controls). We analyzed the response to ROT of all genes differentially expressed with age (FDR-corrected $p < 0.05$, EdgeR and DEseq) detected in comparisons of old versus young controls (brain: 1,436 DEGs, liver: 839, skin: 1,830; Table S17). In Figure 6, these data are shown as 2D plot with $\log_2$ of the expression ratio old controls/young controls on the ordinates and $\log_2$ of the expression ratio old ROT-treated/old controls on the abscissa. In all three tissues, the vast majority (~90%) of genes upregulated during aging were downregulated by ROT and vice versa resulting in highly significant negative regression (Figure 6).

In order to validate these data in a second, longer-living species, the same experiment was repeated in *Danio rerio* (zebrafish). Fish were treated for either 3 or 8 weeks starting at the age of 36 months (approximate median lifespan) (Gerhard et al., 2002; Kishi, 2004) with either vehicle or a concentration of 3.75 nM, that corresponds to 1% of LC_{50} for *D. rerio*. Fish of 12 months treated with vehicle served as young controls. Treatment for 3 weeks resulted in a small number of differentially expressed genes (brain: 39, liver: 208, skin: 89; Table S18) but

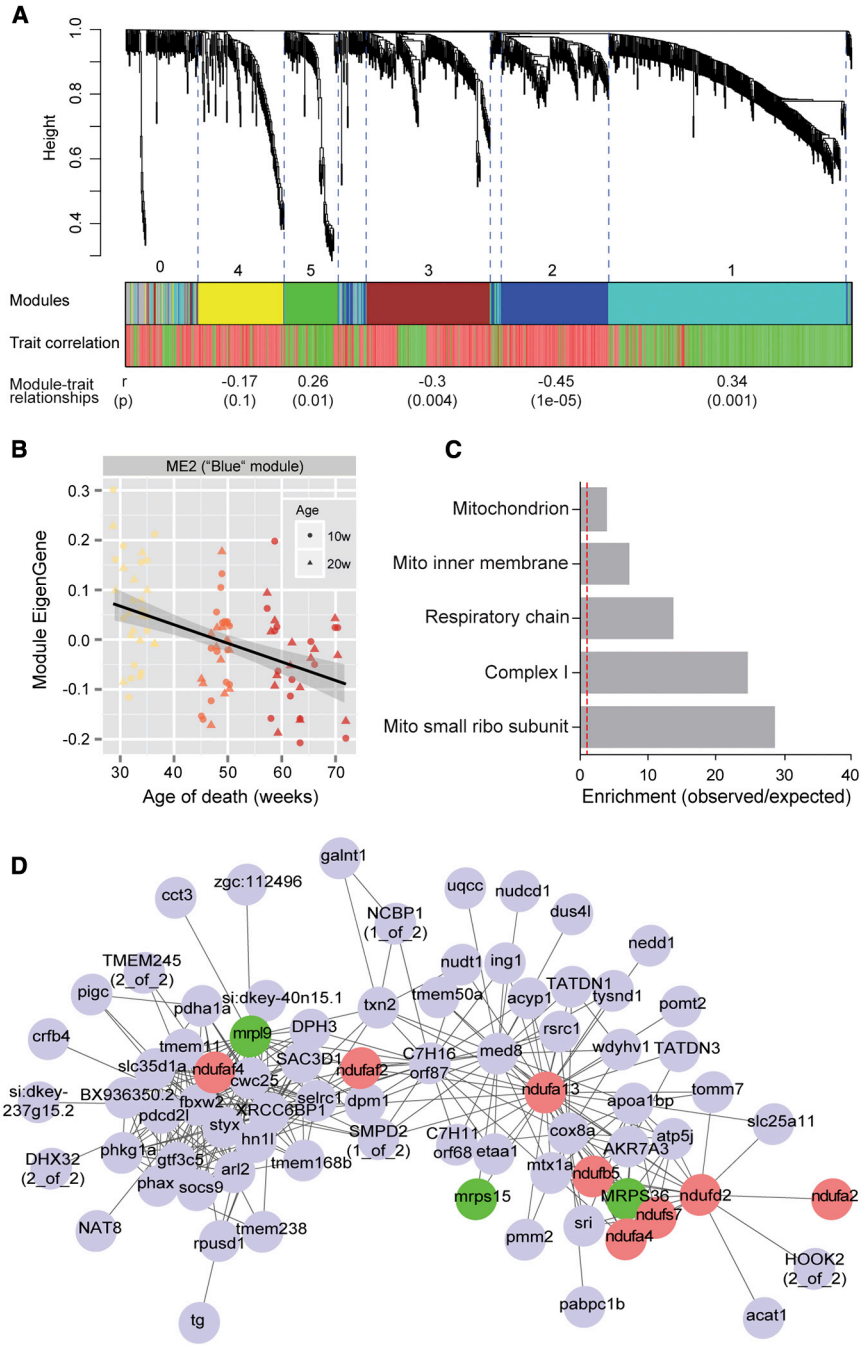

Figure 4. Weighted Gene Co-expression Network Analysis of Genes Correlated with Lifespan

(A) Clustering of the 936 top genes correlated with lifespan. Distance is based on topological overlap. Vertical dotted lines indicate the borders of the different modules that are also indicated by different colors in the horizontal bar. Five clusters containing more than 50 members each were identified. All unclustered genes were dumped into cluster 0. The bottom line indicates the signed correlation of each gene with lifespan: green, positive correlation; red, negative correlation.

(B) Correlation between the eigengene of the "blue" module and the age at death of the individual samples. Circles represent values at 10 weeks and triangles represent values at 20 weeks.

(C) Fold enrichment of gene ontologies in the "blue" module for mitochondrial ontology terms. The red dashed line represents the expected value of 1.

(D) Network of the most connected genes in the "blue" module. Only edges corresponding to topological overlap >0.1 are shown. Genes of complex I are shown in red and mitochondrial ribosomal genes in green.

See also Figure S4 and Tables S14, S15, and S16.

treatment for 8 weeks induced a substantially larger response to ROT in all three tissues (brain: 280 liver: 979, skin: 1,713; Table S19). In *D. rerio*, the majority of genes upregulated during aging were downregulated by ROT and vice versa resulting in highly significant negative regression (Figure 6). This effect was more prominent in the liver (Pearson's r = −0.757, 87% of the genes showing reversal) and least in the skin (r = −0.317, 70% of the genes showing reversal). These data are consistent with a large body of experiments in *C. elegans*, where mitochondrial mutants and RNA interference against genes of the mitochondrial respiratory chain induce life-extension (Dillin et al., 2002b; Kim and Sun, 2007; Lee et al., 2003). Further, it was recently shown that complex I is downregulated during early adult life in the liver of a long-lived mouse strain and in mice under life-long dietary restriction, a condition that prolongs lifespan (Miwa et al., 2014).

DISCUSSION

Here, we have used the short-lived killifish *N. furzeri* to perform a longitudinal study of gene expression during adult life. *N. furzeri* is the shortest-lived vertebrate that can be cultured in captivity and replicates many of the typical hallmarks of aging (reviewed by Cellerino et al., 2015). The recent sequencing of its genome (Reichwald et al., 2015; Valenzano et al., 2015), and the establishment of genome-editing techniques (Harel et al., 2015) makes it a convenient model species for experimental investigations on aging in vertebrates. Here, we report the observation that individual *N. furzeri* of different lifespans differ in their transcript levels at an early adult age. Further, we observed that genome-wide the rate of age-dependent gene modulation was lowest in the longest-lived individuals, suggesting that they are characterized globally by a slower aging rate.

While we suggest that short- and long-lived individuals differ in the baseline and age-dependent modulation of their gene expression at a young age, several confounding factors may contribute to these differences: genetic heterogeneity,

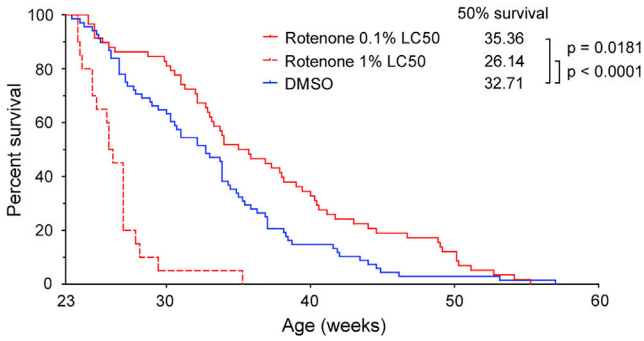

Figure 5. Effects of Rotenone on Lifespan

Survival of rotenone- and vehicle-treated *N. furzeri*; 15 pM rotenone (n = 58, solid red line), 150 pM rotenone (n = 22, dashed red line), and DMSO (n = 47, blue line); p values, log-rank.

differences across the experimental cohorts and differences in the growth parameters. The strain analyzed here shows residual genetic heterogeneity, and we cannot exclude that genetic heterogeneity contributed to lifespan differences in our samples. Alternatively, an obvious explanation for the differences in the rate of age-dependent gene modulation between the lifespan groups could be a higher growth rate (and therefore larger size differences between 10 and 20 week) for the shortest-lived group. We did not detect statistical differences in growth rate between the groups and on the whole population growth was positively, rather than negatively, correlated with lifespan. A similar positive correlation between body size and lifespan was reported in the F2 of a cross between the GRZ and MZM-0403 strains (Kirschner et al., 2012).

The comparison of longitudinal and cross-sectional datasets highlighted ribosomal proteins as upregulated with age in all three tissues and also differentially expressed among the three lifespan groups, so that three groups differ both in the starting values at 10 weeks and the amplitude of age-dependent modulation that is largest in g1 and smallest in g3. Cytosolic ribosomal proteins are also upregulated with age in human brain, kidney, and muscle (Zahn et al., 2006). Very recently, it was shown that in the rat brain, transcription, translation output, and steady-state levels of cytosolic ribosomal proteins are increased upon aging and at the same time expression of mitochondrial ribosomal proteins decreases (Ori et al., 2015), and protein biogenesis machinery is a driver of replicative senescence in yeast (Janssens et al., 2015). Also, the expression of ribosomal proteins is upregulated in *N. furzeri* embryos undergoing diapause (Reichwald et al., 2015), a condition that shows overlaps with aging. Therefore, increased expression of ribosomal proteins appears as a possible conserved biomarker of aging that deserves further functional analysis.

Intuitively, differences in gene expression between individuals that differ in their aging rate should become larger as age progresses. However, we do not observe this consistently as differences between the longevity groups were larger at 10 weeks than at 20 weeks, and numbers of differentially expressed genes between adjacent age steps showed a U-shape. Our observations in *N. furzeri* are rather consistent with the results of a large-scale study of human aging in the prefrontal cortex: rates of age-dependent changes in gene expression are high during childhood, decline until age 20 years, rise again after 40 years, and, by the age of 60, exceed those observed during teenage years (Colantuoni et al., 2011).These observations are reminiscent of the "hourglass" model of comparative embryology. The model, originally proposed to compare the morphology of embryos of different species, postulates that phenotypes are more divergent at early developmental stages, converge at mid-development, and diverge again later. Strong support in favor of this theory came recently from comparison of age-dependent transcriptomes across different species (Casci, 2011). In the human brain, differences in gene expression between areas are largest during prenatal development, decline after birth but, from adolescence onward, differential expression among areas increases again (Pletikos et al., 2014).

The main result of this paper is that conditions favoring longevity are laid out during early adult life when inter-individual differences in gene expression are larger, and this result is consistent with observations in *C. elegans* where knock down of complex I genes or mitochondrial ribosomal proteins during development is necessary and sufficient for life extension. (Dillin et al., 2002a; Houtkooper et al., 2013; Kim and Sun, 2007; Lee et al., 2003).

Reduced mitochondrial mass and function is among the most conserved hallmarks of aging (López-Otín et al., 2013; Zahn and Kim, 2007) and is specifically observed also in *N. furzeri* at the levels of gene expression, mitochondrial mass, and mitochondrial functional parameters (Baumgart et al., 2014; Hartmann et al., 2011). Mitochondrial biogenesis is intimately connected to conserved longevity pathways such as the mTOR- and IGF1-pathways (Bratic and Larsson, 2013). Improved mitochondrial function is currently considered as a crucial component for the health-promoting action of physical exercise and calorie restriction (de Cabo et al., 2014). However, knock down of complex I genes expression induces life-extension in worms and flies (Copeland et al., 2009; Dillin et al., 2002b; Kim and Sun, 2007; Lee et al., 2003). This contradiction between physiological age-dependent regulation and effects observed after genetic manipulations is also observed for another major longevity pathway: the IGF-I pathway. Genetic dampening of IGF-I signaling is life-extending in several models, yet GH and IGF-I hematic concentrations decline during aging (Barzilai et al., 2012). Also, expression of mitochondrial ribosomal proteins declines during aging (de Magalhães et al., 2009; Baumgart et al., 2014; Ori et al., 2015), but knock down of MRPs induces life-extension (Houtkooper et al., 2013).

The effects of ROT may also be explained by the mitohormesis hypothesis postulating that life-extending interventions act via a transient burst of free radical oxygen species that induce adaptive stress responses (Ristow, 2014). In *C. elegans*, life-extending effects of calorie restriction or RNAi of the insulin signaling pathway are blocked by antioxidants (Schmeisser et al., 2013; Schulz et al., 2007; Zarse et al., 2012), and partial inhibition of complex I by ROT prolongs lifespan, generates a burst of ROS, and antioxidants block the life-extending effects of ROT (Schmeisser et al., 2013). Increasing the dosage of ROT, however, is life-shortening in *N. furzeri*, as it is expected by a hormetic effect. Life-extending effects of metformin on mice (Martin-Montalvo et al., 2013) may also be mediated by mitohormesis, since this drug can inhibit complex I (Bridges et al., 2014), and effects of metformin in *C. elegans* were directly linked to mitohormesis via induction of peroxiredoxin (De Haes et al., 2014).

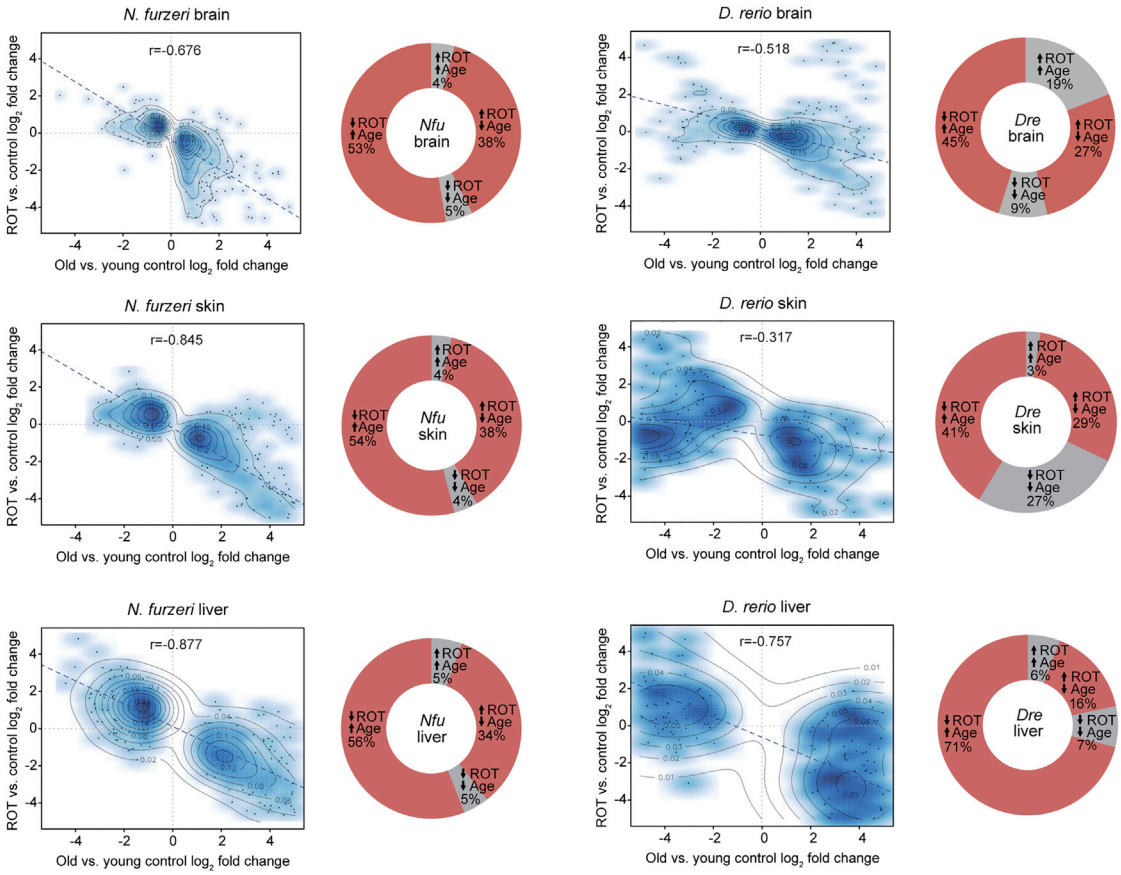

Figure 6. Effects of Rotenone on Gene Expression

Inverse effects of rotenone and age on gene expression in brain, liver, and skin of *N. furzeri* and *D. rerio*. The plots report $\log_2$ fold changes of the union of DEGs between old and young control and between old rotenone-treated and old control. Effect of age is reported on the x axis and effect of rotenone on the y axis. A negative slope of the regression line indicates that the effect of rotenone is opposite the effect of aging. The pie chart indicates the fraction of genes in the different quadrants in clockwise direction from upper right (upregulated with age and ROT) to upper left (down with age and up with ROT); direction of regulation is indicated by arrows.

See also Tables S17, S18, and S19.

We observed that treatment with a dose of ROT three orders of magnitude below the LC_{50} can revert the transcriptional profile of brain, liver, and skin to patterns characteristic of younger animals. This effect was seen not only in *N. furzeri*, but was replicated in *D. rerio*, showing that ROT effects are not linked to the peculiar physiology of this short-lived species. In *D. rerio*, effects of ROT were dependent of the length of treatment: treatment for 3 weeks had a smaller effect than a treatment of 8 weeks. The median lifespan of *D. rerio* is in the order of 3 years (Gerhard, 2003; Herrera and Jagadeeswaran, 2004; Kishi, 2004), therefore 8 weeks represent ~5% of median lifespan indicating that a relatively short treatment can cause rejuvenation of the transcriptome.

In summary, our data suggest complex I as a new potential target for prevention of age-related dysfunctions.

EXPERIMENTAL PROCEDURES

Animal Procedures

The *N. furzeri* strains MZM-0410 and GRZ (provided by Alexander Dorn, Halle, Germany) were studied (Terzibasi et al., 2008). Animal maintenance was performed as described (Terzibasi et al., 2009; Baumgart et al., 2014). The lifespan of 152 single-housed male *N. furzeri* was recorded and tailfin biopsies were taken at 10 weeks and at 20 weeks of age balancing the contribution of the different hatches in the sampling (Table S1). Lethality of rotenone was tested at different dosages for a 96-hr exposure. For long-term treatments, *N. furzeri* and zebrafish were housed in groups. Rotenone was dissolved in DMSO at the needed concentration and pure DMSO was use as control. Drugs were dosed again at each water change. Animal procedures were approved by the local German authority in the State of Thuringia (Veterinaer- und Lebensmittelueberwachungsamt, rotenone treatment: reference number 22-2684-04-03-003/13, longitudinal study: reference number 22-2684-04-03-011/13).

RNA-Sequencing and Analysis

RNA was extracted using Quaziol (QIAGEN). Library preparation using Illumina's TruSeq RNA sample prep kit v2 and sequenced on Illumina HiSeq2500, 50 bp single-read mode in multiplexing obtaining around 50–40 million reads per sample. Read mapping was performed using Tophat 2.0.6 (Kim et al., 2013) and featureCounts v1.4.3-p1 (Liao et al., 2014) using as reference the *N. furzeri* genome (Reichwald et al., 2015) or Zv9.73. DESeq 1.14.0 (Anders and Huber, 2010) and edgeR 3.4.2 (Robinson et al., 2010) were used to identify DEGs for unpaired samples and the intersection of DEGs was assigned as differentially expressed. Paired samples were analyzed with DESeq2 1.4.5

(Love et al., 2014). Differences in fold changes across all the expressed genes in the three groups were tested by ANOVA.

Clustering of Expression Profiles

Genes were clustered according to their temporal profiles using a fuzzy c-means algorithm. We used the function cmeans from the package e1071 1.6-2 of the R programming language. The optimum number of clusters was determined using a combination of several cluster validation indexes as described (Guthke et al., 2005).

Weighted Gene Correlation Network Analysis

Weighted gene correlation network analysis (WGCNA) analysis was performed using the WGCNA package in R (Langfelder and Horvath, 2008) using the unsigned correlation as option and setting the minimum cluster size to 50 members Input for WGCNA was a list of 936 genes showing a significant correlation with lifespan after Benjamini-Hochberg correction.

Gene Set Enrichment Analysis and Gene Ontology

We used the R package gage 2.12.0 (Luo et al., 2009) in order to find significantly enriched KEGG pathways and gene ontology (GO) terms and DAVID v6.7 (Huang et al., 2007a, 2007b) for analysis of gene modules.

ACCESSION NUMBERS

The accession numbers for the data reported in this paper are GEO: GSE52462, GSE66362, and GSE66712.

SUPPLEMENTAL INFORMATION

Supplemental Information includes Supplemental Experimental Procedures, four figures, and nineteen tables and can be found with this article online at http://dx.doi.org/10.1016/j.cels.2016.01.014.

AUTHOR CONTRIBUTIONS

M.B., N.H., M.R., C.E., M.P., and A.C. conceived and designed the study. M.B. performed the *N. furzeri* experiments. N.H. performed the zebrafish experiment. M.G. performed the RNA-seq. S.P., U.M., L.P., and R.G. performed data analysis. P.K. and M.F. performed the variation analysis. A.C. wrote the manuscript with contributions from all other authors.

ACKNOWLEDGMENTS

We thank Sabine Matz, Christin Hahn, Ivonne Heinze, and Ivonne Goerlich for technical assistance and Giorgio Bianchini for drawing. This work was partially supported by the German Ministry for Education and Research (JenAge; BMBF, support codes: 0315581A and 0315581C) and by intramural grant of Scuola Normale Superiore.

Received: July 30, 2015
Revised: November 5, 2015
Accepted: January 29, 2016
Published: February 24, 2016

REFERENCES

Anders, S., and Huber, W. (2010). Differential expression analysis for sequence count data. Genome Biol. *11*, R106.

Bartke, A. (2011). Single-gene mutations and healthy ageing in mammals. Philos. Trans. R. Soc. Lond. B Biol. Sci. *366*, 28–34.

Barzilai, N., Huffman, D.M., Muzumdar, R.H., and Bartke, A. (2012). The critical role of metabolic pathways in aging. Diabetes *61*, 1315–1322.

Baumgart, M., Groth, M., Priebe, S., Savino, A., Testa, G., Dix, A., Ripa, R., Spallotta, F., Gaetano, C., Ori, M., et al. (2014). RNA-seq of the aging brain in the short-lived fish N. furzeri - conserved pathways and novel genes associated with neurogenesis. Aging Cell *13*, 965–974.

Beekman, M., Blanché, H., Perola, M., Hervonen, A., Bezrukov, V., Sikora, E., Flachsbart, F., Christiansen, L., De Craen, A.J., Kirkwood, T.B., et al.; GEHA consortium (2013). Genome-wide linkage analysis for human longevity: Genetics of Healthy Aging Study. Aging Cell *12*, 184–193.

Bratic, A., and Larsson, N.G. (2013). The role of mitochondria in aging. J. Clin. Invest. *123*, 951–957.

Bridges, H.R., Jones, A.J., Pollak, M.N., and Hirst, J. (2014). Effects of metformin and other biguanides on oxidative phosphorylation in mitochondria. Biochem. J. *462*, 475–487.

Broer, L., Buchman, A.S., Deelen, J., Evans, D.S., Faul, J.D., Lunetta, K.L., Sebastiani, P., Smith, J.A., Smith, A.V., Tanaka, T., et al. (2015). GWAS of longevity in CHARGE consortium confirms APOE and FOXO3 candidacy. J. Gerontol. A Biol. Sci. Med. Sci. *70*, 110–118.

Casci, T. (2011). Development: Hourglass theory gets molecular approval. Nat. Rev. Genet. *12*, 76.

Cellerino, A., Valenzano, D.R., and Reichard, M. (2015). From the bush to the bench: the annual Nothobranchius fishes as a new model system in biology. Biol. Rev. Camb. Philos. Soc. Published online April 28, 2015.

Colantuoni, C., Lipska, B.K., Ye, T., Hyde, T.M., Tao, R., Leek, J.T., Colantuoni, E.A., Elkahloun, A.G., Herman, M.M., Weinberger, D.R., and Kleinman, J.E. (2011). Temporal dynamics and genetic control of transcription in the human prefrontal cortex. Nature *478*, 519–523.

Copeland, J.M., Cho, J., Lo, T., Jr., Hur, J.H., Bahadorani, S., Arabyan, T., Rabie, J., Soh, J., and Walker, D.W. (2009). Extension of Drosophila life span by RNAi of the mitochondrial respiratory chain. Curr. Biol. *19*, 1591–1598.

de Cabo, R., Carmona-Gutierrez, D., Bernier, M., Hall, M.N., and Madeo, F. (2014). The search for antiaging interventions: from elixirs to fasting regimens. Cell *157*, 1515–1526.

De Haes, W., Frooninckx, L., Van Assche, R., Smolders, A., Depuydt, G., Billen, J., Braeckman, B.P., Schoofs, L., and Temmerman, L. (2014). Metformin promotes lifespan through mitohormesis via the peroxiredoxin PRDX-2. Proc. Natl. Acad. Sci. USA *111*, E2501–E2509.

de Magalhães, J.P., Curado, J., and Church, G.M. (2009). Meta-analysis of age-related gene expression profiles identifies common signatures of aging. Bioinformatics *25*, 875–881.

Deelen, J., Beekman, M., Uh, H.W., Broer, L., Ayers, K.L., Tan, Q., Kamatani, Y., Bennet, A.M., Tamm, R., Trompet, S., et al. (2014). Genome-wide association meta-analysis of human longevity identifies a novel locus conferring survival beyond 90 years of age. Hum. Mol. Genet. *23*, 4420–4432.

Dillin, A., Crawford, D.K., and Kenyon, C. (2002a). Timing requirements for insulin/IGF-1 signaling in C. elegans. Science *298*, 830–834.

Dillin, A., Hsu, A.L., Arantes-Oliveira, N., Lehrer-Graiwer, J., Hsin, H., Fraser, A.G., Kamath, R.S., Ahringer, J., and Kenyon, C. (2002b). Rates of behavior and aging specified by mitochondrial function during development. Science *298*, 2398–2401.

Fontana, L., Partridge, L., and Longo, V.D. (2010). Extending healthy life span–from yeast to humans. Science *328*, 321–326.

Gems, D., and Partridge, L. (2013). Genetics of longevity in model organisms: debates and paradigm shifts. Annu. Rev. Physiol. *75*, 621–644.

Gerhard, G.S. (2003). Comparative aspects of zebrafish (Danio rerio) as a model for aging research. Exp. Gerontol. *38*, 1333–1341.

Gerhard, G.S., Kauffman, E.J., Wang, X., Stewart, R., Moore, J.L., Kasales, C.J., Demidenko, E., and Cheng, K.C. (2002). Life spans and senescent phenotypes in two strains of Zebrafish (Danio rerio). Exp. Gerontol. *37*, 1055–1068.

Guthke, R., Möller, U., Hoffmann, M., Thies, F., and Töpfer, S. (2005). Dynamic network reconstruction from gene expression data applied to immune response during bacterial infection. Bioinformatics *21*, 1626–1634.

Harel, I., Benayoun, B.A., Machado, B., Singh, P.P., Hu, C.K., Pech, M.F., Valenzano, D.R., Zhang, E., Sharp, S.C., Artandi, S.E., et al. (2015). A platform for rapid exploration of aging and diseases in a naturally short-lived vertebrate. Cell *160*, 1013–1026.

Hartmann, N., Reichwald, K., Wittig, I., Dröse, S., Schmeisser, S., Lück, C., Hahn, C., Graf, M., Gausmann, U., Terzibasi, E., et al. (2011). Mitochondrial DNA copy number and function decrease with age in the short-lived fish Nothobranchius furzeri. Aging Cell *10*, 824–831.

Herndon, L.A., Schmeissner, P.J., Dudaronek, J.M., Brown, P.A., Listner, K.M., Sakano, Y., Paupard, M.C., Hall, D.H., and Driscoll, M. (2002). Stochastic and genetic factors influence tissue-specific decline in ageing C. elegans. Nature *419*, 808–814.

Herrera, M., and Jagadeeswaran, P. (2004). Annual fish as a genetic model for aging. J. Gerontol. A Biol. Sci. Med. Sci. *59*, 101–107.

Houtkooper, R.H., Mouchiroud, L., Ryu, D., Moullan, N., Katsyuba, E., Knott, G., Williams, R.W., and Auwerx, J. (2013). Mitonuclear protein imbalance as a conserved longevity mechanism. Nature *497*, 451–457.

Huang, D.W., Sherman, B.T., Tan, Q., Collins, J.R., Alvord, W.G., Roayaei, J., Stephens, R., Baseler, M.W., Lane, H.C., and Lempicki, R.A. (2007a). The DAVID Gene Functional Classification Tool: a novel biological module-centric algorithm to functionally analyze large gene lists. Genome Biol. *8*, R183.

Huang, D.W., Sherman, B.T., Tan, Q., Kir, J., Liu, D., Bryant, D., Guo, Y., Stephens, R., Baseler, M.W., Lane, H.C., and Lempicki, R.A. (2007b). DAVID Bioinformatics Resources: expanded annotation database and novel algorithms to better extract biology from large gene lists. Nucleic Acids Res. *35*, W169–W175.

Janssens, G.E., Meinema, A.C., González, J., Wolters, J.C., Schmidt, A., Guryev, V., Bischoff, R., Wit, E.C., Veenhoff, L.M., and Heinemann, M. (2015). Protein biogenesis machinery is a driver of replicative aging in yeast. eLife *4*, 4.

Kim, Y., and Sun, H. (2007). Functional genomic approach to identify novel genes involved in the regulation of oxidative stress resistance and animal lifespan. Aging Cell *6*, 489–503.

Kim, D., Pertea, G., Trapnell, C., Pimentel, H., Kelley, R., and Salzberg, S.L. (2013). TopHat2: accurate alignment of transcriptomes in the presence of insertions, deletions and gene fusions. Genome Biol. *14*, R36.

Kirschner, J., Weber, D., Neuschl, C., Franke, A., Böttger, M., Zielke, L., Powalsky, E., Groth, M., Shagin, D., Petzold, A., et al. (2012). Mapping of quantitative trait loci controlling lifespan in the short-lived fish Nothobranchius furzeri–a new vertebrate model for age research. Aging Cell *11*, 252–261.

Kishi, S. (2004). Functional aging and gradual senescence in zebrafish. Ann. N Y Acad. Sci. *1019*, 521–526.

Langfelder, P., and Horvath, S. (2008). WGCNA: an R package for weighted correlation network analysis. BMC Bioinformatics *9*, 559.

Lee, S.S., Lee, R.Y., Fraser, A.G., Kamath, R.S., Ahringer, J., and Ruvkun, G. (2003). A systematic RNAi screen identifies a critical role for mitochondria in C. elegans longevity. Nat. Genet. *33*, 40–48.

Liao, Y., Smyth, G.K., and Shi, W. (2014). featureCounts: an efficient general purpose program for assigning sequence reads to genomic features. Bioinformatics *30*, 923–930.

López-Otín, C., Blasco, M.A., Partridge, L., Serrano, M., and Kroemer, G. (2013). The hallmarks of aging. Cell *153*, 1194–1217.

Love, M.I., Huber, W., and Anders, S. (2014). Moderated estimation of fold change and dispersion for RNA-seq data with DESeq2. Genome Biol. *15*, 550.

Luo, W., Friedman, M.S., Shedden, K., Hankenson, K.D., and Woolf, P.J. (2009). GAGE: generally applicable gene set enrichment for pathway analysis. BMC Bioinformatics *10*, 161.

Martin-Montalvo, A., Mercken, E.M., Mitchell, S.J., Palacios, H.H., Mote, P.L., Scheibye-Knudsen, M., Gomes, A.P., Ward, T.M., Minor, R.K., Blouin, M.J., et al. (2013). Metformin improves healthspan and lifespan in mice. Nat. Commun. *4*, 2192.

Miwa, S., Jow, H., Baty, K., Johnson, A., Czapiewski, R., Saretzki, G., Treumann, A., and von Zglinicki, T. (2014). Low abundance of the matrix arm of complex I in mitochondria predicts longevity in mice. Nat. Commun. *5*, 3837.

Ori, A., Toyama, B.H., Harris, M.S., Bock, T., Iskar, M., Bork, P., Ingolia, N.T., Hetzer, M.W., and Beck, M. (2015). Integrated transcriptome and proteome analyses reveal organ-specific proteome deterioration in old rats. Cell Syst. *1*, 224–237.

Pincus, Z., Smith-Vikos, T., and Slack, F.J. (2011). MicroRNA predictors of longevity in Caenorhabditis elegans. PLoS Genet. *7*, e1002306.

Pletikos, M., Sousa, A.M., Sedmak, G., Meyer, K.A., Zhu, Y., Cheng, F., Li, M., Kawasawa, Y.I., and Sestan, N. (2014). Temporal specification and bilaterality of human neocortical topographic gene expression. Neuron *81*, 321–332.

Rea, S.L., Wu, D., Cypser, J.R., Vaupel, J.W., and Johnson, T.E. (2005). A stress-sensitive reporter predicts longevity in isogenic populations of Caenorhabditis elegans. Nat. Genet. *37*, 894–898.

Reichwald, K., Petzold, A., Koch, P., Downie, B.R., Hartmann, N., Pietsch, S., Baumgart, M., Chalopin, D., Felder, M., Bens, M., et al. (2015). Insights into sex chromosome evolution and aging from the genome of a short-lived fish. Cell *163*, 1527–1538.

Ristow, M. (2014). Unraveling the truth about antioxidants: mitohormesis explains ROS-induced health benefits. Nat. Med. *20*, 709–711.

Robinson, M.D., McCarthy, D.J., and Smyth, G.K. (2010). edgeR: a Bioconductor package for differential expression analysis of digital gene expression data. Bioinformatics *26*, 139–140.

Schmeisser, S., Priebe, S., Groth, M., Monajembashi, S., Hemmerich, P., Guthke, R., Platzer, M., and Ristow, M. (2013). Neuronal ROS signaling rather than AMPK/sirtuin-mediated energy sensing links dietary restriction to lifespan extension. Mol. Metab. *2*, 92–102.

Schulz, T.J., Zarse, K., Voigt, A., Urban, N., Birringer, M., and Ristow, M. (2007). Glucose restriction extends Caenorhabditis elegans life span by inducing mitochondrial respiration and increasing oxidative stress. Cell Metab. *6*, 280–293.

Shen, E.Z., Song, C.Q., Lin, Y., Zhang, W.H., Su, P.F., Liu, W.Y., Zhang, P., Xu, J., Lin, N., Zhan, C., et al. (2014). Mitoflash frequency in early adulthood predicts lifespan in Caenorhabditis elegans. Nature *508*, 128–132.

Singer, T.P., and Ramsay, R.R. (1994). The reaction sites of rotenone and ubiquinone with mitochondrial NADH dehydrogenase. Biochim. Biophys. Acta *1187*, 198–202.

Terzibasi, E., Valenzano, D.R., Benedetti, M., Roncaglia, P., Cattaneo, A., Domenici, L., and Cellerino, A. (2008). Large differences in aging phenotype between strains of the short-lived annual fish Nothobranchius furzeri. PLoS ONE *3*, e3866.

Terzibasi, E., Lefrançois, C., Domenici, P., Hartmann, N., Graf, M., and Cellerino, A. (2009). Effects of dietary restriction on mortality and age-related phenotypes in the short-lived fish Nothobranchius furzeri. Aging Cell *8*, 88–99.

Valdesalici, S., and Cellerino, A. (2003). Extremely short lifespan in the annual fish *Nothobranchius furzeri*. Proc. Biol. Sci. *270* (*Suppl 2*), S189–S191.

Valenzano, D.R., Terzibasi, E., Cattaneo, A., Domenici, L., and Cellerino, A. (2006a). Temperature affects longevity and age-related locomotor and cognitive decay in the short-lived fish Nothobranchius furzeri. Aging Cell *5*, 275–278.

Valenzano, D.R., Terzibasi, E., Genade, T., Cattaneo, A., Domenici, L., and Cellerino, A. (2006b). Resveratrol prolongs lifespan and retards the onset of age-related markers in a short-lived vertebrate. Curr. Biol. *16*, 296–300.

Valenzano, D.R., Benayoun, B.A., Singh, P.P., Zhang, E., Etter, P.D., Hu, C.K., Clément-Ziza, M., Willemsen, D., Cui, R., Harel, I., et al. (2015). The African turquoise killifish genome provides insights into evolution and genetic architecture of lifespan. Cell *163*, 1539–1554.

Willcox, B.J., Donlon, T.A., He, Q., Chen, R., Grove, J.S., Yano, K., Masaki, K.H., Willcox, D.C., Rodriguez, B., and Curb, J.D. (2008). FOXO3A genotype is strongly associated with human longevity. Proc. Natl. Acad. Sci. USA *105*, 13987–13992.

Zahn, J.M., and Kim, S.K. (2007). Systems biology of aging in four species. Curr. Opin. Biotechnol. *18*, 355–359.

Zahn, J.M., Sonu, R., Vogel, H., Crane, E., Mazan-Mamczarz, K., Rabkin, R., Davis, R.W., Becker, K.G., Owen, A.B., and Kim, S.K. (2006). Transcriptional profiling of aging in human muscle reveals a common aging signature. PLoS Genet. *2*, e115.

Zahn, J.M., Poosala, S., Owen, A.B., Ingram, D.K., Lustig, A., Carter, A., Weeraratna, A.T., Taub, D.D., Gorospe, M., Mazan-Mamczarz, K., et al. (2007). AGEMAP: a gene expression database for aging in mice. PLoS Genet. *3*, e201.

Zarse, K., Schmeisser, S., Groth, M., Priebe, S., Beuster, G., Kuhlow, D., Guthke, R., Platzer, M., Kahn, C.R., and Ristow, M. (2012). Impaired insulin/IGF1 signaling extends life span by promoting mitochondrial L-proline catabolism to induce a transient ROS signal. Cell Metab. *15*, 451–465.

Zhang, B., and Horvath, S. (2005). A general framework for weighted gene co-expression network analysis. Stat. Appl. Genet. Mol. Biol. *4*, Article17.